Published in final edited form as:
Mol Immunol. 2013 October ; 55(0): 337–344. doi:10.1016/j.molimm.2013.03.010.

Stereo-selective binding of monoclonal antibodies to the poly-gamma-D-glutamic acid capsular antigen of *Bacillus anthracis*

Mark A. Hubbard[a,c], **Peter Thorkildson**[a], **William H. Welch**[b], and **Thomas R. Kozel**[a,c,*]

[a]Department of Microbiology and Immunology, University of Nevada School of Medicine, Reno, Nevada, 89557 USA

[b]Department of Biochemistry and Molecular Biology, University of Nevada School of Medicine, Reno, Nevada, 89557 USA

[c]Cellular and Molecular Biology Graduate Program, University of Nevada School of Medicine, Reno, Nevada, 89557 USA

Abstract

Bacillus anthracis is surrounded by an anti-phagocytic capsule that is entirely composed of γ-linked D-glutamic acid (γDPGA). γDPGA is required for virulence and is produced in large quantities following spore germination. We have previously described the isolation of several γDPGA-reactive mAbs. The reagents are effective in both immunoprotection and diagnostic applications. The current work was done to further investigate the specificity of γDPGA-reactive mAbs. The specificity of each mAb was characterized using surface plasmon resonance. Our results indicate that each mAb is stereoselective for binding to D-glutamic acid oligomers, but to varying degrees. In particular, mAb F26G3 is highly selective for γDPGA; alterations in stereochemistry disrupted recognition. These differences in mAb reactivity suggest that binding of γDPGA by mAb F26G3 is more specific than non-directional ionic interactions between a negatively charged antigen and a positively charged antibody.

Keywords

antibody; anthrax; polyglutamic acid capsule; stereoselective; molecular model

1. Introduction

Bacillus anthracis is the causative agent of anthrax and a category A biothreat. Virulent strains are encapsulated by a polymer of γ-linked D-glutamic acid (γDPGA), a structure that is unusual among human pathogens (Hanby and Rydon, 1946; Haurowitz and Bursa, 1949; Avakyan et al., 1965; reviewed in Candela and Fouet, 2006). Capsule formation begins immediately upon spore germination, and presents a major obstacle to the mammalian host response (Zwartouw and Smith, 1956; Maynell and Maynell, 1964; Wang and Lucas, 2004; Drysdale et al., 2005). We previously reported that γDPGA is detectable in serum in both murine and non-human primate models of pulmonary anthrax using a monoclonal antibody

*Corresponding author: Department of Microbiology and Immunology/320, University of Nevada School of Medicine, Reno, NV 89557 USA. Phone: 1-775-784-4124. Fax: 1-775-327-2332. tkozel@medicine.nevada.edu.

(mAb)-based immunoassay (Kozel et al., 2004; Kozel et al. 2007; Boyer et al. 2009). Current diagnosis of anthrax is time-consuming and requires the isolation of bacteria by culture. It is likely that novel targets for immunoassay, such as the bacterial capsule, will allow for a rapid diagnosis and, subsequently, reduce mortality through early treatment (Sweeney et al., 2011).

Specificity is a key requirement for diagnostic assays. With anthrax, the intrinsic properties of the capsule present a unique obstacle. Whereas many targets for immunoassay are globular proteins, γ_DPGA is flexible, polyvalent, and carries a significant negative charge. Others have demonstrated that antibodies may bind with high specificity to small peptide targets (Landsteiner and van der Scheer, 1929; Hofstetter et al., 1999), however, previous reports found antibody recognition of γ_DPGA to be more generalized. Studies done by Goodman and colleagues demonstrated that rabbit polyclonal antibody (pAb) generated against whole cells of *B. anthracis* may additionally react with small peptide antigens that incorporate aspartic acid, alanine, and lysine (Goodman and Nitecki, 1966). Furthermore, Goodman noted that anti-capsular pAb did not distinguish between D- and L-isomers of glutamic acid, or polymers that were linked via the β- or γ-carboxyl moieties. Together, these observations contributed to the hypothesis that antibody recognition of polyglutamic acids relied less on the orientation of the carboxyl moieties, and more on the overall secondary and tertiary structural features of the antigen.

Given the results of previous studies that used pAb, it was of interest to determine the binding specificity of several mAbs that react with the *B. anthracis* capsular antigen. To accomplish our analysis, we surveyed binding of four capsule-reactive mAbs to polyglutamic acids that were enantiomerically pure (D- or L-homopeptides). All four mAbs preferentially bound γ_DPGA, however, the results identified a spectrum of mAb specificities, likely due to antigen flexibility and polyvalence. Notably, mAb F26G3 displayed a remarkable preference for γ_DPGA both in strength of binding and the total number of antigen:antibody complexes that were measurable on a twenty-five residue peptide. Together, these results indicate that antibody interactions with poly-glutamic acids are highly dependent on antigen stereochemistry.

2. Materials and Methods

2.1 mAb production

The Immunization protocols for production and isolation of the murine antibodies F24F2 (IgG3), F24G7 (IgG3), F26G3 (IgG3), and F26G4 (IgG3) have been described (Kozel et al., 2004). Hybridoma cell lines were cloned by limiting dilution. mAb-secreting cell lines were grown in tissue culture in an Integra CL 1000 culture flask (Integra Biosciences, East Dundee, IL), and mAbs were isolated by affinity chromatography on protein A (Pierce, Rockford, IL).

2.2 Poly-glutamic acid

γ_DPGA and γ_LPGA polypeptides were synthesized by the Nevada Proteomics Center (University of Nevada, Reno) from 9-fluorenylmethoxy carbonyl-D or L-glutamic acid (O-t-butyl) (Bachem, Peninsula Laboratories, San Carlos, CA) using 9-fluorenylmethoxy carbonyl chemistry. The peptides were purified to approximately 95% using a C_8 YMC column on a Thermo Separations (San Jose, CA) P4000 preparative liquid chromatograph.

2.3 Surface plasmon resonance - affinity determination

Binding experiments were performed using surface plasmon resonance (SPR) with a BIAcore ×100 instrument (GE Healthcare, Piscataway, NJ). The running and sample buffer

for all experiments was HBS buffer, pH 7.4, containing 10 mM HEPES, 150 mM NaCl, 3 mM EDTA, and 0.05% surfactant P20 (HBS-EP+). For ligand preparation, 10 mg of γ_DPGA or γ_LPGA oligomers (25 residues) were biotinylated by standard amine coupling chemistry (Pierce, Rockford, IL) and purified by size exclusion chromatography (Pierce Rockford, IL). Biotinylated peptides were immobilized onto a SA sensor chip until immobilization levels of 80–90 response units (RU) were reached (GE Healthcare). A flow cell was left unmodified for reference subtraction. To evaluate binding, mAb samples were diluted in HBS-EP+ and analyzed at concentrations of 5–333 nM (γ_DPGA) and 26–833 nM (γ_LPGA). At each concentration, mAb was injected over the modified chip surface at 30 μl/min for 180 s. The chip surface was regenerated between runs with a 1 min pulse of 2 M $MgCl_2$. Affinity constants were determined using the 3-parameter Hill equation in Sigma Plot software. A plot of the double reciprocals of binding by all mAbs (1/C versus $1/R_{max}$) gave a regression that was linear (data not shown).

2.4 Surface plasmon resonance - competition assays

Inhibition assays were performed by incubating each mAb (8.3 nM) with a five-residue isopeptide of γ_DPGA or γ_LPGA at 37°C for 1 h. Inhibitor concentrations ranged from 16–500 μM. Following incubation, binding of each sample to a sensor surface immobilized with a twenty five-residue isopeptide of γ_DPGA was analyzed. The percentage inhibition was calculated from a comparison with binding signal achieved by mAb alone. The concentration of free peptide required for 50% inhibition of mAb binding (IC_{50}) was calculated by a hyperbolic regression analysis using SigmaPlot software. The inhibition constant (K_I) was calculated using: $K_I = IC_{50}/(1 + ([C]/K_D))$ (Cheng Y and Prusoff WH, 1973).

2.5 Molecular model

2.5.1 Computational methods

The model was constructed de novo taking advantage of the well-defined repetitive domain structure of immunoglobulins (Ig). Each two-chain domain was constructed individually. The template of the structurally conserved region (SCR) of each chain was selected from candidates identified from FUGUE (de Bakker et al., 2001; Shi, Blundell, and Mizugchi, 2001; Williams et al., 2001) ORCHESTRAR, as implemented in SYBYL (Tripos Inernational, St. Louis, MO.) and FASTA (Berman et al., 2000) searches of the Protein Data Bank (www.rsb.org).

The amino acid sequence of the template was converted to that of the target using the spl (SYBYL) script “atomic horror.” Gaps and insertions in the SCR were repaired by the SYBYL loop search utility. Side chains were relaxed. As necessary, the two chains comprising the folding domain were docked using the PDB template files as guides. The structure was refined using molecular dynamics constrained by fixed distance, range distance, and torsion constraints. The search loop algorithm was applied to repair gaps that remained in the loop regions (from insertions and deletions). Constrained molecular dynamics was reapplied. The four folding domains were assembled into Fab and Fc fragments. The initial docks were guided by Ig structures deposited in the PDB and subsequently refined by the docking program HEX (Ritchie and Venkatraman, 2010). The assembled Fab and Fc domains were refined by constrained molecular dynamics (MD). Sequence gaps were repaired by the loop search algorithm and refined by constrained MD. Constrained MD was applied first in continuum solvent followed by extensive MD in explicit solvent (TIP3). Finally, unconstrained MD was applied. The AMBER force field was used throughout the MD simulations.

The quality of the target structure was accessed by a variety of statistical comparisons with experimentally determined Ig structures. These tests include i) configuration of peptide bonds, ii) Ramachandran plots, iii) side chain rotomer probability, iv) surface/buried positional probability, and v) strain energy. Only the Fab fragment was used for this report and only to illustrate properties relevant to experimental results reported in this manuscript.

2.5.2 Conformational landscape

The SYBYL software package was used to determine the conformational landscape of γ_DPGA. A peptide of three γ-linked D-glutamyl residues (trimer) was constructed. Here, the end groups were included to simulate the effect of adjacent residues in a larger polymer. The AMBER force-field and charge set were used in MDa simulations; however, both were slightly modified to account for the different geometry. A molecular database of rotamers of the single bonds of the backbone (N-Cα, Cα-Cβ, Cβ-Cγ, Cγ-Cδ) of the central residue was constructed through the use of a conformational search algorithm. Using molecular mechanics (steepest descent and Powell minimizers, no simplex) each conformer was minimized in two stages. First the terminal residues were relaxed and then the entire trimer was relaxed.

3. Results

3.1 Affinity measurements by SPR

A panel of mAbs that are reactive with the capsular polypeptide of *B. anthracis* (γ_DPGA) has been described (Kozel et al., 2007). The mAbs resulted from immunization of BALB/c mice with soluble capsule that was isolated from *Bacillus licheniformis* culture supernatant fluids. Unlike *B. anthracis*, which produces a capsule of enantiomerically pure γ_DPGA, *B. licheniformis* incorporates a varied content of D- and L-glutamic acids to its capsular filaments. The relative proportion of D- and L-glutamic acids may be altered through the addition of metal cations (Leonard CG, Housewright RD, and Thorne CB, 1958). The purified capsule of *B. licheniformis* that was used for the generation of the present mAb library consisted of ~84% D-glutamic acid.

The mixed content of the immunizing agent raises questions as to the true specificity of the library of γ_DPGA mAbs. To determine the specificity, each mAb was first assayed to establish its binding affinity with oligomers of synthesized, enantiomerically pure γ_DPGA The analysis was done using SPR. The binding surface was prepared by direct immobilization of biotinylated γ_DPGA oligomer (25 residues, 25mer) to a streptavidin-coated sensor chip. Total immobilization of γ_DPGA 25mer was 80 RU. In the SPR platform, binding response is a function of weight located on the sensor surface (1000 RU = 1 ng/mm^2). Therefore, it is possible to calculate the total antigen density of the immobilized surface. At 80 RU, the predicted average distance between γ_DPGA 25mer is 82 Å. This distance is approximately the same as the known Stokes radius of an IgG, which is 75 Å. The distance between γ_DPGA molecules is large enough to permit binding of at least 1 mAb to each antigen, yet small enough for interactions to occur among bound mAbs. A titratable increase in RU was observed following a 180 s pulse of each mAb concentration (Fig. 1). A regression analysis of RU versus mAb concentration found that all mAbs bound to γ_DPGA with nano molar affinity (Fig. 2). The calculated binding strengths displayed a hierarchy that was evident but subtle, placing F24F2≈F26G3>F26G4>F24G7. The difference in γ_DPGA-binding affinity between the strongest (F26G3) and weakest (F24G7) binders was 11:34 nM or ΔG = 700 cal/mol; equivalent to the loss or gain of up to two hydrogen bonds. The observed range in affinity constants was also accompanied by a hierarchy in the total amount of mAb on the sensor chip surface at saturation (RU_{max}), indicating variability in total mAb:Ag complexes formed on the sensor surface (F24G7>F26G4≈F26G3≈F24F2).

These differences were also subtle. The highest ratio of mAb per γ_DPGA molecule was 2.7 (F24G7); in comparison, the lowest ratio was 1.8 (F24F2) (Table 1).

Each mAb was also assayed for reactivity with enantiomerically pure γ_LPGA 25mer. The amount of γ_LPGA that was immobilized to a sensor chip was 90 RU, which corresponds to 78 Å between each antigen molecule. Initial studies that used the identical mAb concentrations in the evaluation of binding to the γ_DPGA 25mer surface displayed limited reactivity (data not shown). A nearly 10-fold increase in mAb concentration, as compared to γ_DPGA experiments, was required to obtain useful binding data (Fig. 1). Interaction of the four mAbs with immobilized γ_LPGA was quite different when compared to γ_DPGA. All mAbs displayed larger dissociation constants and lower RU_{max}, but at variable magnitudes. MAb F26G4 bound to γ_LPGA with a dissociation constant of 160 nM. In contrast, mAbs F24F2, F24G7 and F26G3 bound γ_LPGA with markedly lower affinities of 260, 260, and 280 nM, respectively. When compared to γ_DPGA binding, these differences accounted for 8–23 fold changes in dissociation constants or ΔG = 1.3–1.9 Kcal/mol. Stark differences were also observed in the saturation densities of mAb on the γ_LPGA sensor surface, as was evidenced by the lower RU_{max} values. MAbs F24G7 and F26G4 saturated the chip surface at relatively higher densities of 4400 and 4500 RU, respectively. Lower saturation densities were observed in mAb F24F2 (1300 RU) and, more strikingly, mAb F26G3 (300 RU). The calculated ratio of mAb per γ_LPGA molecule ranged from 1 (mAbs F24G7 and F26G4) to ~0.1 (mAbs F24F2 and F26G3) (Table 1).

3.2 Competitive assays

Binding inhibition experiments were also performed to further investigate the activity of mAbs in our library. We wanted to determine if binding specificity was influenced by the state of the antigen, i.e. solid versus fluid phase. It is possible that fluid-phase antigen may assume conformations not found in the solid phase, and that such conformations are reactive with the mAb-binding site. Alternatively, it can be hypothesized that epitope accessibility may be hindered by direct immobilization to the sensor surface. To this end, experiments were designed such that mAb binding to a γ_DPGA-immobilized sensor chip could be inhibited after incubation with a soluble ligand.

Initially, a fixed concentration of each mAb (8.3 nM) was pre-incubated with free γ_DPGA 5mer in varying concentration (16–500 μM) before injection over a γ_DPGA-immobilized sensor surface. The mAb concentration of 8.3 nM was chosen as it was either at or below the calculated K_D of all four mAbs. All mAbs were inhibited from binding to solid phase γ_DPGA 25mer by the presence of soluble γ_DPGA 5mer but at varying degrees (Fig. 4). MAb F26G3 bound free-γ_DPGA with an inhibition constant (K_I) of 48 μM. In contrast, mAbs F24F2, F24G7, and F26G4 displayed increased K_I values of 73, 98, and 340 μM, respectively. These trends were similar to the previous direct-binding experiments, which showed a weaker affinity for mAb F24G7 as compared to the others. The study was repeated by incubating each mAb with free γ_LPGA 5mer. Analysis showed that binding to the γ_DPGA-coated sensor surface was not affected by the presence of the soluble γ_LPGA peptide, even when excess inhibitor concentrations were present (500 μM) (Fig. 4).

Additional studies with mAb F26G3 were done to assess the effect of polymer length on antibody recognition. A previous study found that five glutamyl residues optimally fill the antibody binding pocket (Kozel et al., 2007). Larger peptides, therefore, may be used to determine if contacts are made outside the binding pocket; such contacts may contribute to specificity. To this end, 10- and 25-residue length γ_D- or γ_LPGA peptides were assayed for inhibition activity. Using ten times the K_I, a complete loss of surface binding was observed for γ_DPGA inhibitors. However, identical amounts of γ_LPGA were insufficient to inhibit

binding to surface-associated γ_DPGA when using either the 10- and 25-residue peptides (data not shown).

3.3 Molecular Modeling

MAb F26G3 was chosen for the creation of a molecular model. The model is intended to illustrate the nature of γ_DPGA-mAb interactions. Homology modeling was used to create a representation of the F26G3 binding pocket. The VH and VL CDRs were introduced to the structurally conserved regions obtained from template structures deposited in the RCSB PDB. Conformational minimization was performed to obtain a low-energy structure. Molecular dynamics simulations were used to visualize interactions between the mAb and γ_DPGA. The solvent accessible surface area (SASA) of the binding pocket is shown in Fig. 5, along with the mAb residues that have contact with the antigen at four-angstroms. These residues are present on both the heavy and light chains and include Tyr, Trp, Ala, His, Lys, and Arg. Finally, the model shows that five $_D$-glutamyl residues occupy the binding site, this observation is consistent with previous experimental data (Kozel et al., 2007).

The number of possible conformations in the γ_DPGA backbone was estimated by exploring the conformational space of a three residue γ-$_D$-glutamyl molecule. The highly flexible propionate side chain connecting the amides of γ-$_D$-glutamate has a theoretical 81 conformers; four single bonds each with three rotational energy minima. A conformational search algorithm was used to generate a database of conformers. These were then minimized using molecular mechanics. For each γ-$_D$-glutamate monomer, 28 conformers were found within 1.4 kcal/mol of the global energy minimum.

The effect of mAb-binding on antigen mobility was assessed. Antigen mobility was measured as the radius of gyration (ROG) using molecular dynamics simulation. A γ_DPGA 25mer was docked to mAb F26G3. The ROG was measured for the five γ-$_D$-glutamyl residues within the binding pocket, as well as five unbound γ-$_D$-glutamyl residues on the far side of the polymer. The results indicate bound γ_DPGA is less mobile, in comparison to unbound γ_DPGA; <ROG> = 7.1 Å ± 0.3 and <ROG > = 7.4 Å ± 0.5, for bound versus unbound, respectively. Although these values appear similar, qualitative analysis of ROG suggest otherwise (Fig. 6). Here, two conformers, each with a lifetime of 30 ps (<ROG > = 6.8 ± 0.2 and 7.3 ± 0.2) dominate the bound section; in contrast, no stable conformer was detected in the unbound section. Therefore, binding energy is sufficient to restrict the residue motion into identifiable conformers.

4. Discussion

Molecular recognition between antibody and antigen involves interactions among surfaces that are continuously in a state of flux. Binding reactions may involve necessary conformational changes by the antigen or antibody before the formation of the antigen-antibody complex. Alternatively, conformational changes may be necessary within the antigen-antibody complex itself. Here, a flexible bivalent antibody interacts with a flexible, multivalent and highly disordered antigen. Interactions between the two surfaces are, therefore, complex. In this study, mAbs reactive with the capsular polypeptide of *B. anthracis* were assayed for binding activity using surface plasmon resonance, which allows the visualization of antigen-antibody complex formation in realtime, and without chemical reporters. Surface plasmon resonance also facilitates the calculation of the total number of antigen-antibody complexes, as weight is directly proportional to the response signal. Given the length and flexibility of the antigen used in this study (PGA 25mer), it is likely that the antigen-antibody complexes occurred both as a function of inter-antigen (cross-linking between two separate 25mers) and intra-antigen binding.

To estimate the total number binding sites per 25mer filament, the binding response at several mAb concentrations was recorded and extrapolated to predict the theoretical RU_{max} when an infinite amount of mAb is present. Under these conditions, all second order rate processes become infinitely large and first order reactions, such as prior isomerization and induced fit become important. On a γ_DPGA-coated sensor surface, an average of 2 (mAbs F24F2, F26G3, F26G4) to 3 (mAbs F24G7) bound mAbs per individual antigen molecule. This observation is consistent with the polyvalent nature of the antigen, and suggests that a high number of overlapping binding sites are present. This knowledge suggests the likelihood that the total maximum binding for each mAb is not limited by the number of possible epitopes on a single antigen, but the point at which the repulsive interactions between mAbs (molecular crowding) are greater than the attractive energy of binding. We assume that the individual, capsule-reactive mAbs differ in the ability to orient themselves on the sensor surface to promote optimal packing. Because each mAb that was used in this study is a murine IgG3, we can assume that structural differences affecting segmental flexibility are not a factor. Thus, the differences in R_{max} may rely, at least in part, on epitope abundance, accessibility, and orientation.

Prior sequencing data confirmed the variable region of each mAb in this group is unique; however, the four mAbs tested here show remarkable similarity in binding affinities and maximum surface densities for γ_DPGA. Preliminarily, these results suggest that all four mAbs have closely similar epitopes; however, binding of each mAb to γ_LPGA suggests otherwise. Here, for each mAb the density of binding was less and the dissociation constants larger. At saturation; one mAb bound per γ_LPGA 25mer (F24G7 and F26G4), one mAb bound every one in three γ_LPGA 25mer (F24F2), and most strikingly, one mAb bound every one in ten γ_LPGA 25mer (F26G3). We can assume that the conformational flexibility of the γ_LPGA compensates for the difference in stereochemistry; however, the favorable antigen conformers become less abundant and only permit a low density of antibody binding. Interestingly, mAbs F24G7 and F26G4 have the weakest binding to γ_DPGA, and the least ability to discriminate between $_D$- and $_L$-isomers. The relatively smaller changes in affinity (~8 fold for γ_DPGA versus γ_LPGA) and higher saturation densities supports this hypothesis. Most likely, the reduced differences in the binding of γ_DPGA versus γ_LPGA for these mAbs is a consequence of the high flexibility and polyvalent nature of the antigen; such qualities allow for multiple antigen conformers to exist with similar binding energies. Overall, the data suggest that antigen stereochemistry influences both the total amount and energetic favorability of conformers recognized by all mAbs in this library.

Competition experiments offer further insight into antibody binding. Our previous findings indicated that the K_D values of all four γ_DPGA-reactive mAbs were nearly identical (Kozel et al., 2007 and Table 1). These measurements were determined by fluorescence perturbation and relied on alteration of the microenvironment of tryptophan residues found in the binding pocket of each mAb. Such measurements may be used to determine the *intrinsic* affinity of antibody binding, which refers to the strength of a single antigen-antibody interaction in solution. Using a small γ_DPGA 5mer, the intrinsic affinity of each mAb was determined to be ~500 nM. In the current study, the *functional* affinity of each mAb to the surface-bound γ_DPGA was much higher (~10–50×). The increase in functional versus intrinsic affinity that was observed for each mAb is likely due to restriction of antigen flexibility in three-dimensional space and the ability of the antibody to bind the antigen bivalently. In a competitive environment, the mAbs always favored binding to surface-associated over fluid-phase antigen. The large K_I values (48–340 μM) from these experiments support this observation. Interestingly, mAb F24G7 was relatively insensitive to the addition of free γ_DPGA 5mer. Prior experiments using fluorescence perturbation also demonstrated that mAb F24G7 had 2–3 fold lower levels of maximum quenching when compared to the other anti-capsular mAbs (Kozel et al., 2007).

The observation that antibodies reactive with this capsular polypeptide are stereo-*selective* rather than stereo-*specific* is not surprising. The poly-glutamic acid antigen is highly flexible; such antigens present special considerations for molecular recognition. The binding pockets of all mAbs in this study accommodate five-glutamyl peptides. This knowledge was derived experimentally (Kozel et al., 2007) and *in silico* (mAb F26G3) (Fig. 5). Because the backbone of this γ-linked homopolymer contains four rotatable bonds, each residue can theoretically exist in 81 rotamers. A systematic conformation search using a γ_DPGA 3mer confirms that each glutamyl residue exists in a large number of conformers; however, the energies of each conformer are sufficiently different that only a few will be populated at 310K. Here, we calculate the total number to be 28. Therefore, the 5-residue antigen may assume 28^5(or 1.7×10^7) theoretical conformations. It is reasonable, with such numerable conformations possible, that molecular recognition of γ_D- or γ_LPGA may not be completely specific. It is almost certain that a sub-population of conformers from each antigen will highly resemble one another.

The antibody binding pocket may also exist is several conformers; however, the amino acids that make up the complementarity determining regions (CDR) of the antibodies are considerably more restricted in movement than the free polyglutamic acid antigen. For example, the CDRs consist of stretches of amino acids that connect to framework regions in the variable domain. The flexibility of these loop structures are inhibited by the end-to-end distance between two framework regions. As a consequence, the CDR may move freely within the confines of excluded volume and electrostatic energy, but is limited from lateral movement. In contrast, the antigen has no such restrictions and is only limited by excluded volume and electrostatic energy. Additionally, the number of rotatable bonds in each CDR-associated amino acid is two, whereas the number of rotatable bonds in each residue of γ-linked PGA is three. Therefore, we assume for this study that the flexibility of the antigen is more influential than the flexibility of the antibody for the bimolecular interaction; however, this observation is certainly not true for all antigens.

Despite the flexibility and charge-density of the antigen, it is likely that mAb-binding occurs following recognition of a particular epitope and not merely non-directional ionic forces between a negatively charged antigen and a positively charged antibody. Molecular dynamics simulations of a 25mer bound to mAb F26G3 support this hypothesis. Here, the conformational difference between bound and free portions of the antigen were evident. When bound, discrete conformations were observed during time-averaged experiments; these conformations had some of the lowest energies of all possible conformers. The unbound portions of the antigen, however, were considerably more mobile. The differences in the radius of gyration for bound versus unbound antigen illustrate this point (Fig. 6). Notably, unbound antigen displayed increased mean, standard deviation, and range values for radius of gyration, when compared to bound antigen; accordingly, no such stable conformers were identified during time-course experiments. These observations suggest mAb-binding leads to a restriction in antigen flexibility, as contacts between specific residues are critical to the binding interaction.

The molecular model of mAb F26G3 found that 12 residues are in 4Å contact with the antigen. Of these 12 residues, there are: 1-Ala, 2-Arg, 1-His, 2-Lys, 1-Trp and 5-Tyr. Previous reports of amino acid usage in the complementarity determining region (CDR) of antibodies have indicated that Tyr is the most common (~40%) (Zemlin et al., 2003). The Tyr content of mAb F26G3 approximates this value (42%). Overall, Tyr is associated with antibodies that share high complementarity with antigen, as hydrogen bonding and Van der Waals forces are the most prevalent. In contrast, Arg, His, and Lys are uncommon to the CDRs (≤1% usage). Here, these 3 amino acids constitute 42% of the 4Å contacts as well. Most likely, the overuse of these basic amino acids is a consequence of the acidic nature of

the antigen. Molecular modeling reveals the formation of specific salt-bridges between the antibody and antigen, which supports this hypothesis. Finally, the presence of Arg in the binding pocket is associated with reduction in antigen specificity (Birtalan et al., 2008). This finding supports our observation that the binding pocket is selective, but not specific for γ_DPGA.

Overall, the current study highlights the ability of mAbs to discern between nearly identical structures. Previous observations concluded that polyclonal antibodies show little selectivity for enantiomers of polyglutamic acids. Evaluation of our mAb library yielded similar results with mAbs F24G7 and F26G4, both exhibiting a subtle preference for γ_DPGA. In contrast, mAbs F24F2 and, in particular, F26G3 were more selective for γ_DPGA. In practical terms, this degree of specificity may be advantageous in reagent selection for the construction of immunoassays to detect the capsular antigen of *B. anthracis*.

Acknowledgments

This work was supported by Public Health Service grants R01AI059348 and R01AI093365 from the National Institutes of Allergy and Infectious Diseases (TRK).

Glossary

γ_DPGA	γ-linked $_D$-polyglutamic acid
γ_LPGA	γ-linked $_L$-polyglutamic acid
mAb	monoclonal antibody
pAb	polyclonal antibody
SPR	surface plasmon resonance
K_I	inhibition constant
K_D	dissociation constant

References

AuCoin DP, Sutherland MD, Percival AL, Lyons CR, Lovchik JA, Kozel TR. Rapid detection of the poly-gamma-d-glutamic acid capsular antigen of *Bacillus anthracis* by latex agglutination. Diagn Microbiol Infect Dis. 2009; 64:229–232. [PubMed: 19345041]

Berman HM, Westbrook J, Feng Z, Gilliland G, Bhat TN, Weissig H, Shindyalov IN, Bourne PE. The Protein Data Bank. Nuc Acid Res. 2000; 28:235–242.

Birtalan S, Zhang Y, Fellouse FA, Shao L, Schaefer G, Sindhu SS. The intrinsic contributions of tyrosine, serine, glycine and arginine to the affinity and specificity of antibodies. J Mol Biol. 2008; 377:1518–1528. [PubMed: 18336836]

Boyer AE, Quinn CP, Hoffmaster AR, Kozel TR, Saile E, Marston CK, Percival A, Plikaytis BD, Woolfitt AR, Gallegos M, Sabourin P, McWilliams LG, Pirkle JL, Barr JR. Kinetics of lethal factor and poly-d-glutamic acid antigenemia during inhalational anthrax in rhesus macaques. Infect Immun. 2009; 77:3432–3441. [PubMed: 19506008]

Candela T, Fouet A. *Bacillus anthracis* CapD, belonging to the gamma-glutamyltranspeptidase family, is required for the covalent anchoring of capsule to peptidoglycan. Mol Microbiol. 2005; 57:717–726. [PubMed: 16045616]

Candela T, Fouet A. Poly-gamma-glutamate in bacteria. Mol Microbiol. 2006; 60:1091–1098. Review. [PubMed: 16689787]

Cheng Y, Prusoff WH. Relationship between the inhibition constant (K1) and the concentration of inhibitor which causes 50 per cent inhibition (I50) of an enzymatic reaction. Biochem Pharmacol. 1973; 22:3099–3108. [PubMed: 4202581]

de Bakker PI, Bateman A, Burke DF, Miguel RN, Mizuguchi K, Shi J, Shirai H, Blundell TL. HOMSTRAD: adding sequence information to structure-based alignments of homologous protein families. Bioinform. 2001; 17:748–749.

Drysdale M, Heninger S, Hutt J, Yahua C, Lyons CR, Koehler TM. Capsule synthesis by *Bacillus anthracis* is required for dissemination in murine inhalational anthrax. The EMBO Journal. 2005; 24:221–227. [PubMed: 15616593]

Dutta P, Tipple CA, Lavrik NV, Datskos PG, Hofstetter H, Hofstetter O, Sepaniak MJ. Enantioselective sensors based on antibody-mediated nanomechanics. Anal Chem. 2003; 75:2342–2348. [PubMed: 12918975]

Goodman JW, Nitecki DE. Immunochemical studies on the poly-γ-D-glutamyl capsule of *Bacillus anthracis*. I. Characterization of the polypeptide and of the specificity of its reaction with rabbit antisera. Biochem J. 1966; 5:657–665.

Hanby WE, Rydon HN. The capsular substance of *Bacillus anthracis* . Biochem J. 1946; 40:297–309.

Haurowitz F, Bursa F. The linkage of glutamic acid in protein molecules. Biochem J. 1949; 40:297–307.

Hofstetter H, Cary JR, Eleniste PP, Hertweck JK, Lindstrom HJ, Ranieri DI, Smith GB, Undesser LP, Zeleke JM, Zeleke TK, Hofstetter O. New developments in the production and use of stereoselective antibodies. Chirality. 2005; 17:S9–S18. [PubMed: 15612044]

Hofstetter O, Hofstetter H, Wilchek M, Schurig M, Green BS. Chiral discrimination using an immunosensor. Nat Biotech. 1999; 17:371–374.

Hofstetter O, Hofstetter H. Antibodies as chiral selectors for the determination of enantioenrichment. Enantiomer. 2001; 6:153–158. [PubMed: 11570421]

Inglesby TV, O'Toole T, Henderson DA, Bartlett JG, Ascher MS, Eitzen E, Friedlander AM, Gerberding J, Hauer J, Hughes J, McDade J, Osterholm MT, Parker G, Perl TM, Russell PK, Tonat K. Working group on civilian biodefense Anthrax as a biological weapon, 2002: updated recommendations for management. JAMA. 2002; 287:2236–2252. Review. [PubMed: 11980524]

Janse I, Hamidjaja RA, Bok JM, van Rotterdam BJ. Reliable detection of *Bacillus anthracis,Francisella tularensis* and *Yersinia pestis* by using multiplex qPCR including internal controls for nucleic acid extraction and amplification. BMC Microbiol. 2010; 10:314. [PubMed: 21143837]

Kocianova S, Vuong C, Yao Y, Voyich JM, Fischer ER, DeLeo FR, Otto M. Key role of poly-gamma-dl-glutamic acid in immune evasion and virulence of *Staphylococcus epidermidis* . J Clin Invest. 2005; 115:688–694. [PubMed: 15696197]

Kozel TR, Murphy WJ, Brandt S, Blazar BR, Lovchik JA, Thorkildson P, Percival A, Lyons CR. mAbs to *Bacillus anthracis* capsular antigen for immunoprotection in anthrax and detection of antigenemia. Proc Nat Acad Sci. 2004; 101:5042–5047. [PubMed: 15051894]

Kozel TR, Thorkildson P, Brandt S, Welch WH, Lovchik JA, AuCoin DP, Vilai J, Lyons CR. Protective and immunochemical activities of monoclonal antibodies reactive with the *Bacillus anthracis* polypeptide capsule. Infect Immun. 2007; 75:152–163. [PubMed: 17060470]

Landsteiner K, van der Scheer J. Serological differentiation of steric isomers. J Exp Med. 1928; 48:315–320. [PubMed: 19869486]

Leonard CG, Housewright RD, Thorne CB. Effects of some metallic ions on glutamyl polypeptide synthesis by *Bacillus subtilis* . J Bacteriol. 1958; 76:499–503. [PubMed: 13598708]

Makino S, Watarai M, Cheun HI, Shirahata T, Uchida I. Effect of the lower molecular capsule released from the cell surface of *Bacillus anthracis* on the pathogenesis of anthrax. J Infect Dis. 2002; 186:227–233. [PubMed: 12134259]

Meynell E, Meynell GG. The roles of serum and carbon dioxide in capsule formation by *Bacillus anthracis* . J Gen Microbiol. 1964; 34:153–164. [PubMed: 14121214]

Ritchie DW, Venkatraman V. Ultra-fast FFT protein docking on graphics processors. Bioinformatics. 2010; 26:2398–2405. [PubMed: 20685958]

Shi J, Blundell TL, Mizuguchi K. FUGUE: sequence-structure homology recognition using environment-specific substitution tables and structure-dependent gap penalties. J Mol Biol. 2001; 310:243–257. (2001). [PubMed: 11419950]

Silvaieh H, Schmid MG, Hofstetter O, Schurig V, Gübitz G. Development of enantioselective chemiluminescence flow- and sequential-injection immunoassays for alpha-amino acids. J Biochem Biophys Methods. 2002; 53:1–14. [PubMed: 12406581]

Sweeney DA, Hicks CW, Cui X, Li Y, Eichacker PQ. Anthrax infection. Am J Respir Crit Care Med. 2011; 184:1333–1341. [PubMed: 21852539]

Wang TT, Lucas AH. The capsule of *Bacillus anthracis* behaves as a thymus-independent type 2 antigen. Infect Immun. 2004; 72:5460–5463. [PubMed: 15322045]

Williams MG, Shirai H, Shi J, Nagendra HG, Mueller J, Mizuguchi K, Miguel RN, Lovell SC, Innis CA, Deane CM, Chen L, Campillo N, Burke DF, Blundell TL, de Bakker PI. Sequence-structure homology recognition by iterative alignment refinement and comparative modeling. Proteins. 2001; (Suppl. 5):92–97. [PubMed: 11835486]

Zanuy D, Alemán C, Muñoz-Guerra S. On the helical conformation of un-ionized poly(gamma-d-glutamic acid). Int J Biol Macromol. 1998; 23:175–184. [PubMed: 9777704]

Zemlin M, Klinger M, Link J, Zemlin C, Bauer K, Engler JA, Schroeder HW, Kirkham PM. Expresssed murine and human CDR-H3 intervals of equal length exhibit distinct repertoires that differ in their amino acid composition and predicted range structures. J Mol Biol. 2003; 334:733–749. [PubMed: 14636599]

Zwartouw HT, Smith H. Polyglutamic acid from *Bacillus anthracis* grown *in vivo*: structure and agressin activity. Biochem J. 1956; 63:437–442. [PubMed: 13341899]

Highlights

- We determined the binding affinities and specificities of several murine mAbs that react with the capsule of *Bacillus anthracis*.
- Binding of all mAbs was not solely dependent on non-directional ionic forces.
- All mAbs preferentially bound γ-linked D glutamic acid over γ-linked L glutamic acid.
- The murine mAb F26G3 was the most selective for γ-linked D glutamic acid.
- A molecular model of mAb F26G3 shows five glutamic acid residues optimally fill the binding site and that two conformations have 30 picosecond lifetimes.

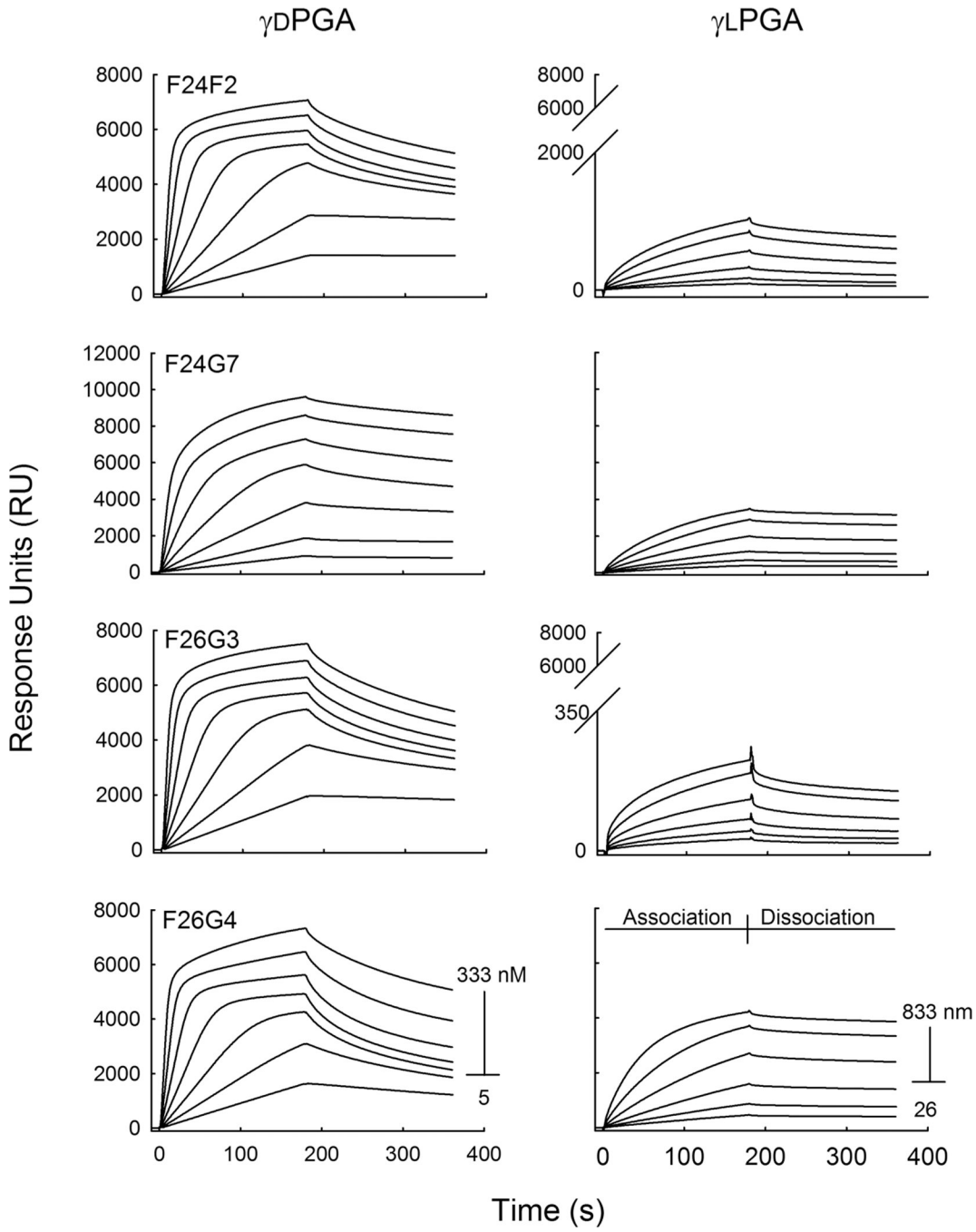

Fig. 1.

Binding specificity of anti-capsular mAbs. Synthetic γ_D- and γ_LPGA 25mer were immobilized to separate sensor chips at 80 and 90 RU, respectively. mAb binding was analyzed in a two-fold dilution series at a mAb concentration of 5.5–333 nM to the γ_DPGA coated surface (left), and at a mAb concentration range of 26–833 nM to the γ_LPGA coated surface (right). The corresponding sensorgrams are given as a function of response generated over time for each mAb concentration. Note the substantial differences in the magnitude of response for binding of D versus L antigens.

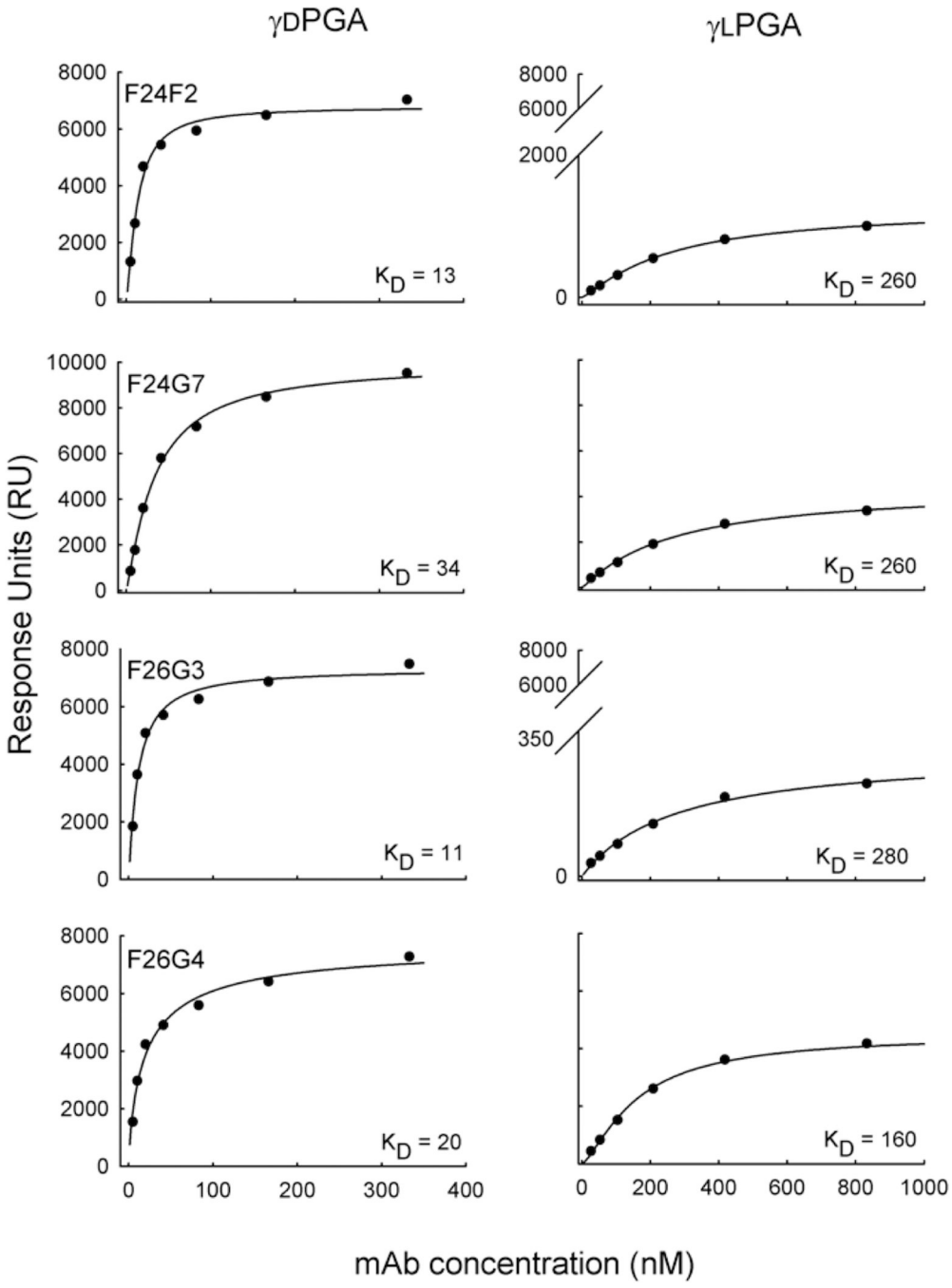

Fig. 2.

Binding affinity of anti-capsular mAbs to γ_D- and γ_LPGA-coated surfaces by surface plasmon resonance. The total RU that was achieved on each surface following a 180 s pulse is given as a function of mAb concentration. The 3-parameter Hill equation was used to create the regression line. The dissociation constants of each mAb were determined as: $y = ax^b/(c^b+x^b)$, where c equals the apparent dissociation constant (K_D).

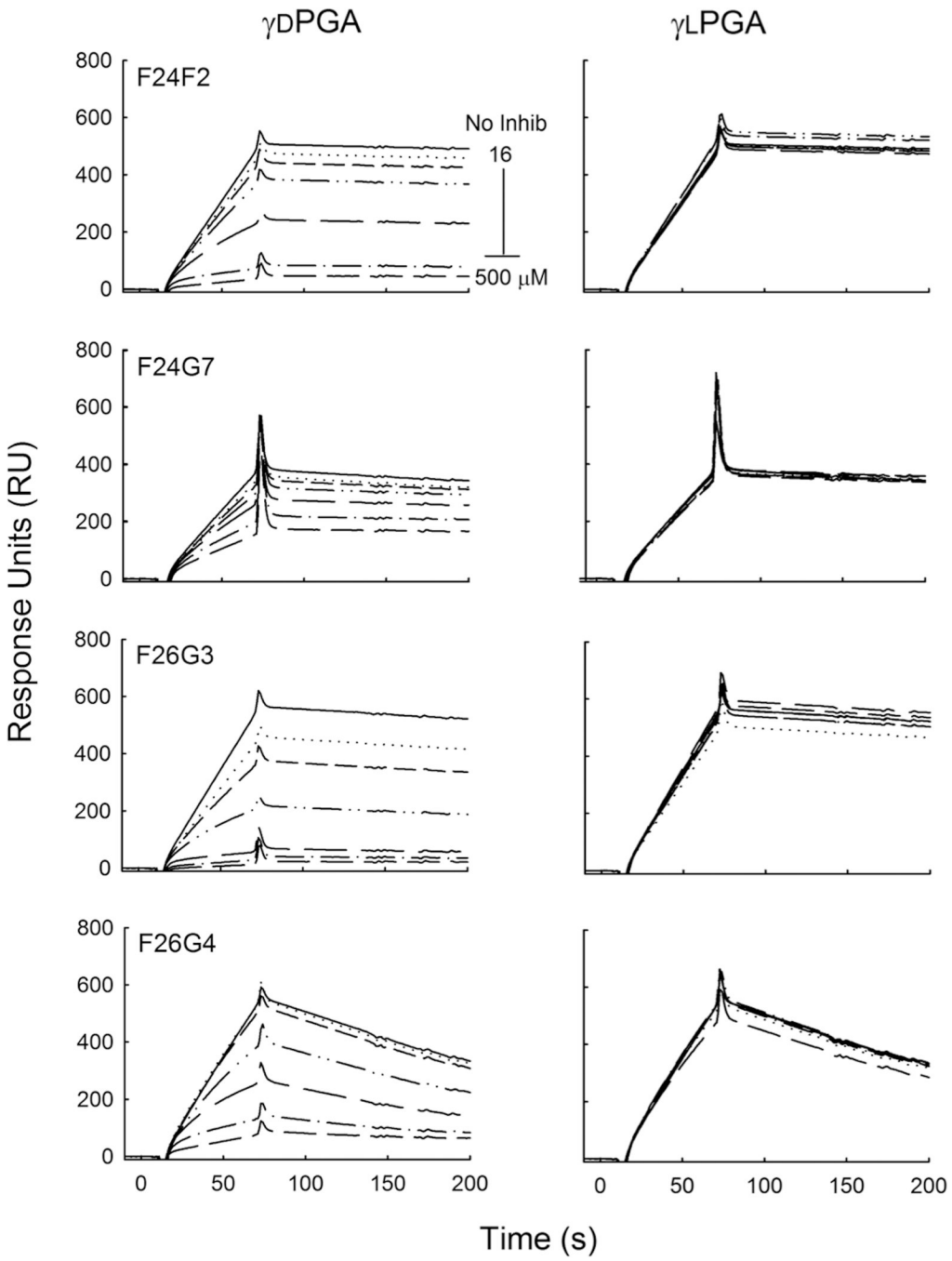

Fig. 3.

Competition assays using short peptide inhibitors. A single concentration of each capsule-reactive mAb was incubated with synthetic oligopeptide (5 residue) of either γ_DPGA (left) or γ_LPGA (right). Concentrations of the inhibitors ranged from 16–500 μM in a two-fold dilution series. The binding of mAb:inhibitor mixtures were analyzed by a 60 s pulse over a γ_DPGA-immobilized sensor chip.

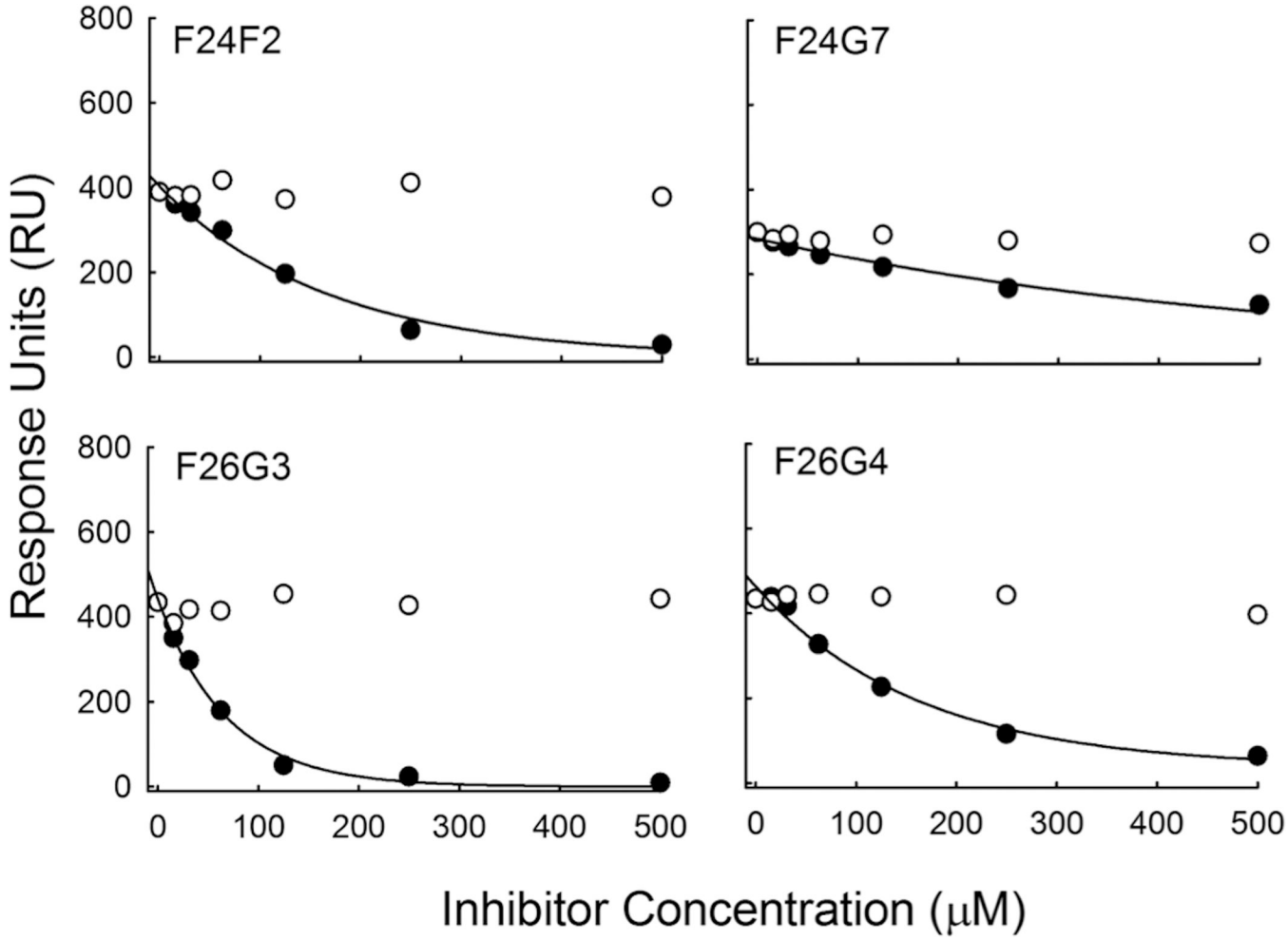

Fig. 4.

Determination of inhibition constants. Binding response is given as a function of inhibitor concentration.The closed circles represent γ_DPGA 5mer, whereas the open circles represent the γ_LPGA 5mer. A titratable decrease in RU was not observed in any of the capsule-reactive mAbs when a γ_LPGA inhibitor was present. Hyperbolic fits of the inhibition that was observed with soluble γ_DPGA were used to calculate the concentration of inhibitor necessary to achieve a fifty percent signal decrease (IC_{50}). IC_{50} values were then used to derive the K_I value for each mAb.

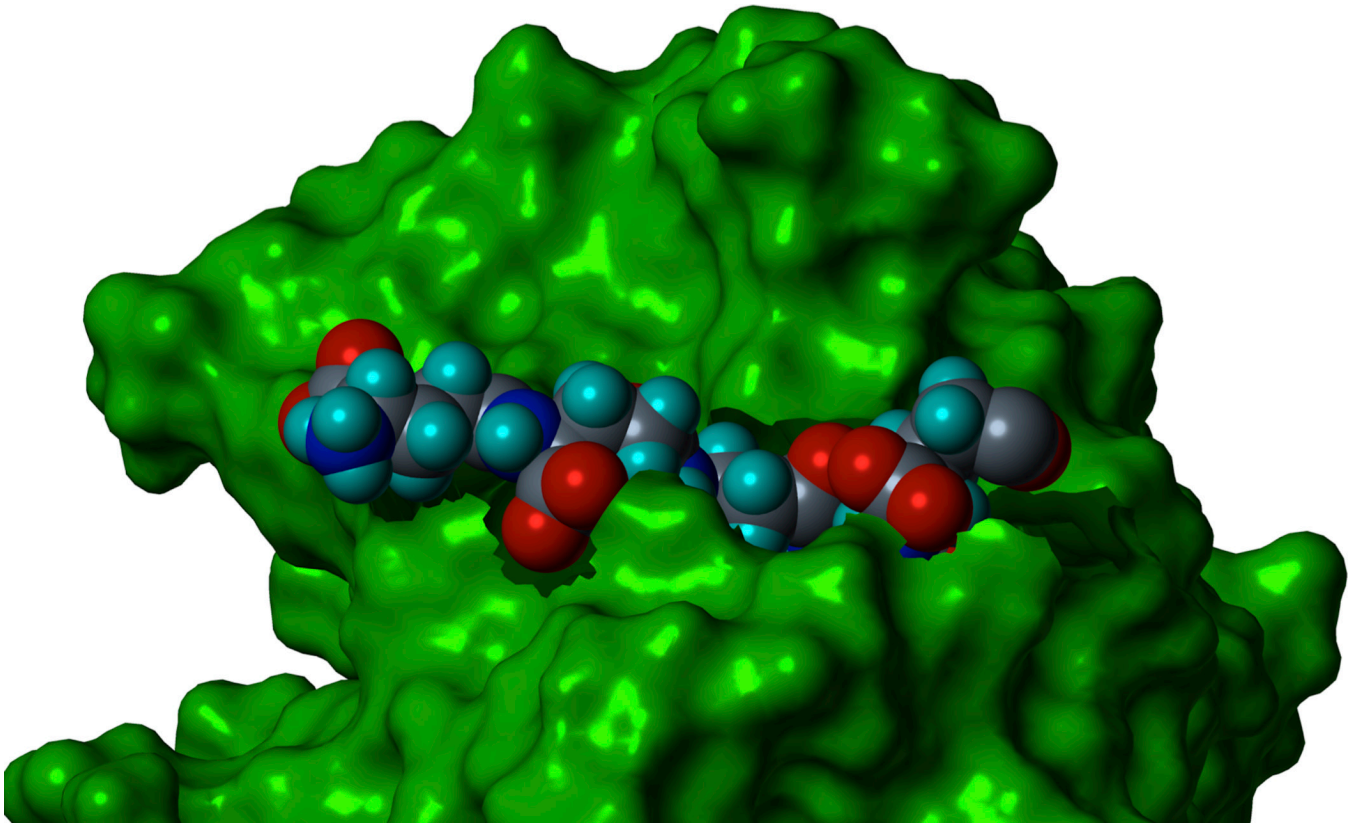

Fig. 5.

The binding pocket of mAb F26G3. The solvent accessible surface of the binding pocket is shown in green. Additionally, a single γ_DPGA 5mer is shown in space-fill with hydrogen, carbon, nitrogen, and oxygen being represented in white, grey, blue, and red, respectively. Docking simulations show that 5 γ-glutamyl residues optimally fill the binding pocket.

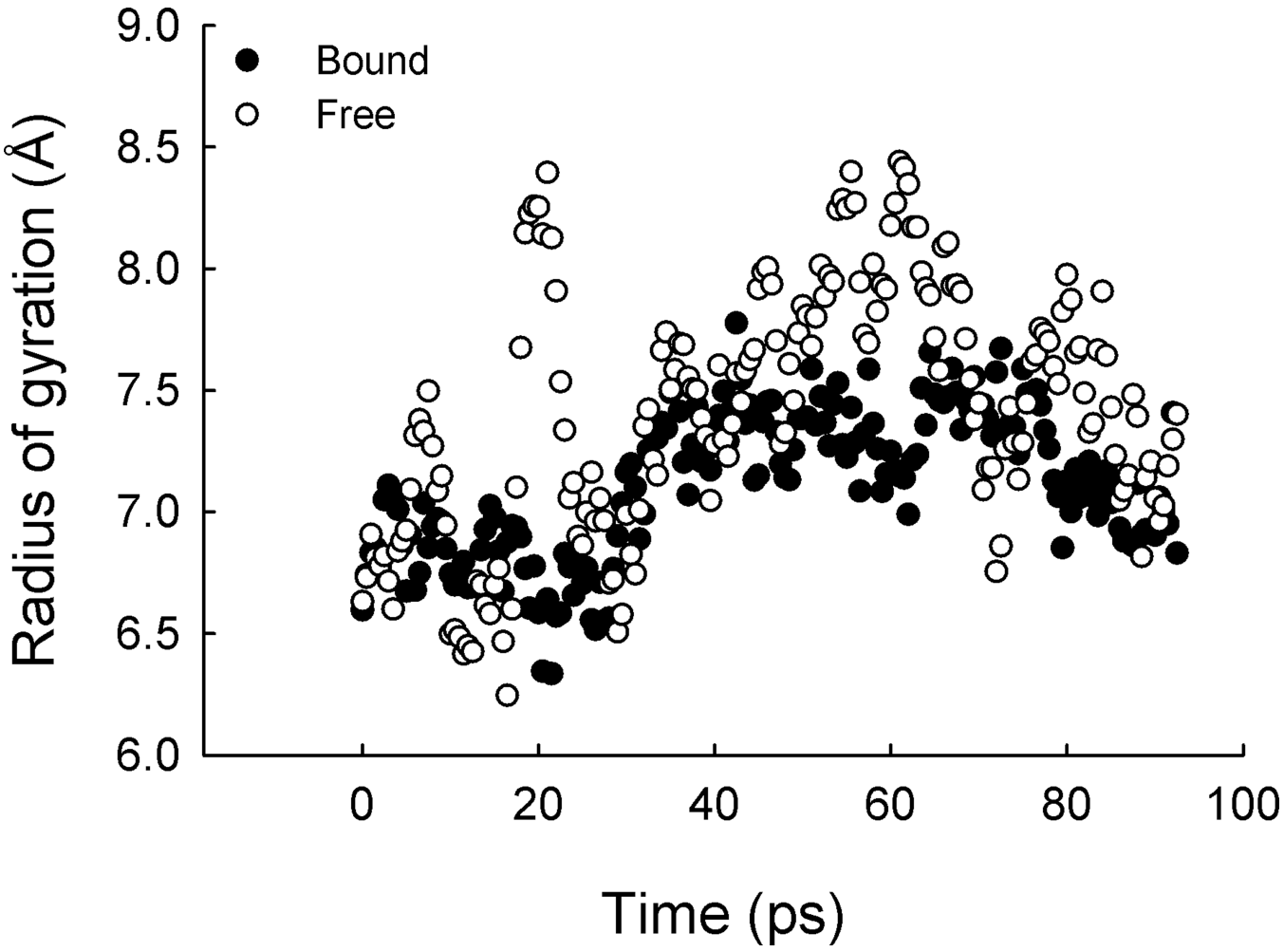

Fig. 6.

Mobility of mAb-bound and free γDPGA. Molecular dynamic simulation was used to analyze the difference of antigen mobility in the bound a free states. A γDPGA 25mer was docked to mAb F26G3. The five γD-glutamyl peptides in the binding pockets were measured for lateral mobility using the radius of gyration (closed circles). Alternatively, five γD-glutamyl peptides on the unbound portion of the 25mer were measured for comparison (open circles). Note the restriction in movement.

Table 1

Binding and immunochemical properties of anti-capsular mAbs

		γDPGA					γLPGA				
mAb	**Subclass**	**K_D [a]**	**K_D [b]**	**K_I [c]**	**RU_{max}**	**mAb:Ag**	**K_D [d]**	**K_D [b]**	**K_I [c]**	**RU_{max}**	**mAb:Ag**
F24F2	IgG3	0.5	13	73	6800	1.8	nt	260	>500	1300	0.3
F24G7	IgG3	0.36	34	340	10000	2.7	nt	260	>500	4000	1.0
F26G3	IgG3	0.37	11	48	7300	2.0	nt	280	>500	300	0.07
F26G4	IgG3	0.51	20	98	7800	2.1	nt	160	>500	4500	1.1

[a] Intrinsic affinity using fluorescence perturbation (μM), results adapted from Kozel et al., 2007

[b] Functional affinity using SPR (nM)

[c] Inhibition constant using fluid and solid phase antigen in SPR format (μM)

[d] Intrinsic affinity using fluorescence perturbation (μM); nt, not tested